Catalysis Today 274 (2016) 22–27

Contents lists available at ScienceDirect

Catalysis Today

journal homepage: www.elsevier.com/locate/cattod

Highly photocatalytic active thiomolybdate $[Mo_3S_{13}]^{2-}$ clusters/Bi_2WO_6 nanocomposites

Dongting Yue, Zichen Zhang, Zheyi Tian, Taiyang Zhang, Miao Kan, Xufang Qian, Yixin Zhao*

School of Environmental Science and Engineering, Shanghai Jiao Tong University, 800 Dongchuan Rd., Shanghai 200240, China

ARTICLE INFO

Article history:
Received 28 October 2015
Received in revised form
28 December 2015
Accepted 19 January 2016
Available online 15 February 2016

Keywords:
Photocatalyst
$Mo_3S_{13}^{2-}/Bi_2WO_6$
$[Mo_3S_{13}]^{2-}$ nanoclusters
Co-catalyst

ABSTRACT

The $Mo_3S_{13}^{2-}/Bi_2WO_6$ nanocomposites were facilely fabricated by depositing $[Mo_3S_{13}]^{2-}$ clusters onto the hydrothermally prepared Bi_2WO_6 nanoparticles. This novel $Mo_3S_{13}^{2-}/Bi_2WO_6$ nanocomposite exhibited unprecedented visible light photocatalytic activities. The deposited $[Mo_3S_{13}]^{2-}$ clusters enhanced the photocatalytic activity of Bi_2WO_6 by promoting the migration of photoinduced charges, which restrained the recombination of photogenerated hole–electron (h^+/e^-) pairs on the surface of Bi_2WO_6. Furthermore, the high photocatalytic stability and recyclability of $Mo_3S_{13}^{2-}/Bi_2WO_6$ nanocomposite enable it to be a promising candidate for the environmental remediation especially in wastewater treatment. In all, $[Mo_3S_{13}]^{2-}$ clusters with advantages of low cost and earth-abundance are great potential as co-catalyst for photocatalysts.

© 2016 Elsevier B.V. All rights reserved.

1. Introduction

The growing global environmental contamination and energy crisis especially in developing country have attracted worldwide attention as threat for sustainable development of human society. Photocatalysis is one of the most promising potential technology candidates for organic pollutants degradation and hydrogen generation because of its low cost, high efficiency and utilization of solar energy [1–6]. Among the various studied photocatalysts, bismuth-based semiconductors (Bi_2MoO_6, Bi_2WO_6, $BiVO_4$, BiOX etc.) exhibit excellent photocatalytic properties with the irradiation of visible light owing to their appropriate band gap in the visible light range, high photostability and low toxicity [7–9]. Among them, Bi_2WO_6 with a suitable band gap energy of ~2.6 eV is regarded as a promising candidate for photo-degrading hardly biodegradable organic contaminants due to its excellent intrinsic physico-chemical properties [10–13]. However, the rapid recombination of photogenerated hole–electron (h^+/e^-) pairs in Bi_2WO_6 seriously limits the energy-conversion efficiency.

It is well known that high photocatalytic efficiency of Bi_2WO_6 can be obtained by controlling morphology to facilitate the charge seperation. Bi_2WO_6 has been synthesized into various nanostructures including nanoparticles, nanorods, nanoplates, sphere-like, flower-like and hollow spheres etc., which exhibit excellent visible light photocatalytic performance for various organic pollutants degradation [14–19]. Although the morphology controlled shape can enhance the photocatalytic properties, the improvement in charge separation remains limited. To address this challenge, many research efforts including heterojunction structure, ions doping, and co-catalyst loading have been invested [3,19–29]. Among these methods, loading co-catalyst has been regarded as an effective and practical approach. The well known platinum (Pt) is widely utilized as the co-catalyst due to its excellent catalytic activities. However, the large scale application of Pt as co-catalysts for photocatalysis is limited its scarcity and high-cost.

Very recently, the low cost and earth-abundance molybdenum sulfide materials (MoS_x) become a promising Pt alternative catalysts in electrochemical applications [30]. In this paper, we have prepared the novel photocatalyst of $Mo_3S_{13}^{2-}/Bi_2WO_6$ nanocomposite. The thiomolybdate $[Mo_3S_{13}]^{2-}$ nanoclusters were facilely deposited onto hydrothermally synthesized Bi_2WO_6 nanoparticles. Typical model pollutant including rhodamine B (RhB) and methylene blue (MB) could be effectively photocatalytic decomposed by $Mo_3S_{13}^{2-}/Bi_2WO_6$ nanocomposites. Our experiments show that $[Mo_3S_{13}]^{2-}$ nanoclusters are an excellant photocatalysts' co-catalysts, which is comparable to Pt. In addition, a possible photocatalytic mechanism on the considerable improvement of $Mo_3S_{13}^{2-}/Bi_2WO_6$ composites is finally proposed.

* Corresponding author.
E-mail address: yixin.zhao@sjtu.edu.cn (Y. Zhao).

http://dx.doi.org/10.1016/j.cattod.2016.01.051
0920-5861/© 2016 Elsevier B.V. All rights reserved.

2. Experimental

2.1. Materials

Bismuth(III) nitrate pentahydrate ($Bi(NO_3)_3{\cdot}5H_2O$), tungstic acid sodium salt (Na_2WO_4), acetic acid (CH_3COOH), ethylenediamine tetraacetic acid disodium salt dihydrate (EDTA-2Na), *tert*-butanol (TBA), benzoquinone (BQ), rhodamine B (RhB), methylene blue (MB), ammonium heptamolybdate tetrahydrate ($(NH_4)_6Mo_7O_{24}{\cdot}4H_2O$), carbon disulfide, toluene and ethanol were analytical pure and were used as received. All of them were purchased from Sinopharm Chemical Reagent Co., Ltd. Polyvinylpyrrolidone (PVP) and barium sulfate were purchased from Aladdin Industrial Corporation. Ammonium polysulfide solution was purchased from Xiya reagent.

2.2. Catalyst preparation

2.2.1. Synthesis of Bi_2WO_6 nanoparticles

Firstly, a 45 mL aqueous solution was prepared by dissolving 0.55 g (1.66 mmol) of Na_2WO_4 and 0.01 g of PVP in deionized (DI) water followed by sonicating in an ultrasonic water bath for 30 min. Secondly, 1.6 g (3.32 mmol) $Bi(NO_3)_3{\cdot}5H_2O$ was dissolved in 45 mL of CH_3COOH with vigorous stirring. Then, two solutions were mixed together and stirred until it became homogeneous. Finally, the mixture solution was transferred into a 150 mL Teflon-lined stainless steel autoclave and was heated at 150 °C for 18 h. The precipitate was obtained by centrifuging and washing with ethanol and DI water for several times, followed by drying at 60 °C for 6 h.

2.2.2. Preparation of $[Mo_3S_{13}]^{2-}$ nanoclusters

The thiomolybdate $(NH_4)_2Mo_3S_{13}{\cdot}nH_2O$ (n = 0–2) was obtained using the method outlined by Kibsgaard et al. [30]. The detailed synthetic process was displayed in Supporting information.

2.2.3. Fabrication of $Mo_3S_{13}^{2-}/Bi_2WO_6$ nanocomposites

$Mo_3S_{13}^{2-}/Bi_2WO_6$ nanocomposites were prepared by following steps. Briefly, 0.1 g of Bi_2WO_6 powder first dispersed in 300 mL of DI water and sonicated for 30 min. Then, different amount of thiomolybdate $(NH_4)_2Mo_3S_{13}{\cdot}nH_2O$ was added into Bi_2WO_6 suspension followed by vigorous stirring at room temperature for 6 h. Finally, the powders were collected, washed with ethanol several times, and then dried at 60 °C. According to this approach, different weight ratios of $(NH_4)_2Mo_3S_{13}{\cdot}nH_2O$ to Bi_2WO_6 composites at 0.0002:1, 0.0005:1, 0.001:1, and 0.002:1 were fabricated and labeled as 0.02 wt% $Mo_3S_{13}^{2-}/Bi_2WO_6$, 0.05 wt% $Mo_3S_{13}^{2-}/Bi_2WO_6$, 0.1 wt% $Mo_3S_{13}^{2-}/Bi_2WO_6$, and 0.2 wt% $Mo_3S_{13}^{2-}/Bi_2WO_6$.

2.3. Characterization and measurements

The X-ray diffraction (XRD) patterns of the samples were obtained using an automated Bruker D8 Advance X-ray diffractometer with Cu-Kα radiation (λ = 1.5406 Å) at 40 kV and 40 mA. The data were recorded at a scan rate of 10° min^{-1} in the 2θ range from 10° to 80°. Fourier transform infrared (FTIR) spectra of the samples were measured on Tensor 27 FTIR spectrometer (Nicolet 6700). The morphologies were characterized with a JEOL-JEM-2100F transmission electron microscope (TEM) and a Sirion 200 field emission scanning electron microscope (FESEM) equipped with an energy-dispersive X-ray spectroscope (EDS). The elemental composition of samples were determined by inductively coupled plasma optical emission spectrometer (ICP-AES, iCAP6300,Thermo). The X-ray photoelectron spectroscopy (XPS) test was performed on a Kratos Axis Ultra^{DLD} spectrometer with a monochromatic Al K_α source (1486.6 eV). All binding energies were referenced to the C 1s peak (284.8 eV) of adventitious carbon on the analyzed sample surface. Diffuse reflectance spectra (DRS) were measured using a Lambda 750 UV–vis-NIR (ultraviolet–visible-near-infrared) spectrophotometer. $BaSO_4$ was used as the reflectance standard material. The band gap energy was calculated referring to Tauc's formula. Photoluminescence (PL) measurements of the $Mo_3S_{13}^{2-}/Bi_2WO_6$ composites were carried out using an excitation wavelength of 300 nm by fluorescence spectrophotometer (F-380, Tianjin Gangdong SCI.&TECH. Development Co., Ltd.). The slit width for the measurements was 10 nm. Powder samples were used without further treatment.

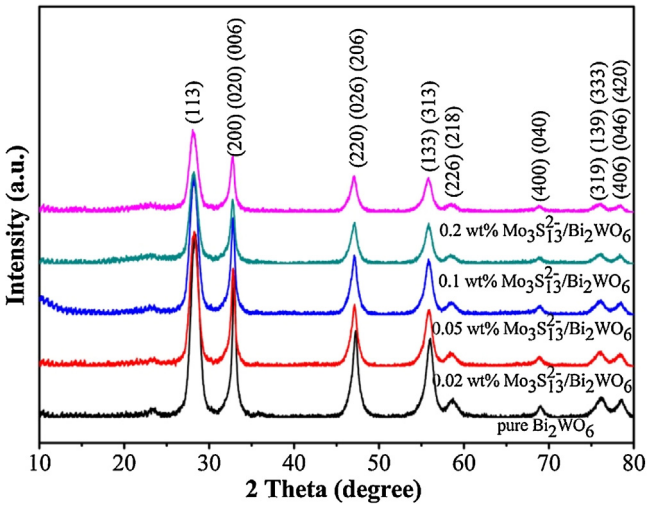

Fig. 1. XRD patterns of pure Bi_2WO_6 and $Mo_3S_{13}^{2-}/Bi_2WO_6$ composites with different mass ratios of $[Mo_3S_{13}]^{2-}$ clusters.

2.4. Photocatalytic processes of RhB and MB

The visible light (λ ≥ 420 nm) photocatalytic activities of the composite powders were evaluated by the degradation of RhB and MB using a 500 W Xe lamp (Ceaulight, CEL-LAX500) with the filter. 5 mg of the samples were added to RhB aqueous solutions (10 mg L^{-1}, 10 mL) and MB aqueous solutions (5 mg L^{-1}, 10 mL), respectively. Before irradiation, the suspension was stirred for 30 min in the dark to reach the adsorption–desorption equilibrium. At given time intervals, 10 mL of the suspensions were taken out and subsequently separated by centrifugation. Then, the filtrates were analyzed by an Agilent Cary 60 to measure the concentration change of reactant and product under the characteristic absorption wavelength of RhB (553 nm) and MB (664 nm). For the regeneration test of the photocatalyst, 5 consecutive cycles of MB were tested, and the samples were washed thoroughly with DI water and dried after each cycle.

3. Results and discussion

The XRD patterns of Bi_2WO_6 and $Mo_3S_{13}^{2-}/Bi_2WO_6$ composites with different content of $[Mo_3S_{13}]^{2-}$ are shown in Fig. 1. The diffraction peaks can be assigned to the phase pure orthorhombic Bi_2WO_6 (JCPDS No. 39-0256) with the most intensive peak of (1 1 3) plane. All the diffraction peaks of the $Mo_3S_{13}^{2-}/Bi_2WO_6$ composites are similar to that of pure Bi_2WO_6, indicating that the introduction of $[Mo_3S_{13}]^{2-}$ does not lead to the formation of new crystal phase or changes in preferential orientations. Since the low weight content and high dispersion of $[Mo_3S_{13}]^{2-}$, no obvious diffraction peaks is corresponded to $(NH_4)_2Mo_3S_{13}{\cdot}nH_2O$ in Fig. S1.

The morphologies and microstructures of samples were investigated by SEM, TEM and HRTEM. The typical SEM image of Bi_2WO_6

Download English Version:

https://daneshyari.com/en/article/53196

Download Persian Version:

https://daneshyari.com/article/53196

Daneshyari.com